Dissociation, Relaxation, and Incubation in the Pyrolysis of Neopentane: Heat of Formation for *tert*-Butyl Radical

N. K. Srinivasan, J. H. Kiefer,* and R. S. Tranter

Department of Chemical Engineering, University of Illinois at Chicago, Chicago, Illinois 60607

Received: October 16, 2002; In Final Form: January 13, 2003

Rate processes in neopentane−krypton mixtures were examined at high temperatures and over a very wide range of pressure in a shock tube using the laser−schlieren technique. The experiments used mixtures of 2, 5, 10, 20, and 30% in Kr and covered 600−2000 K for postshock pressures of 7−400 Torr. The combination of high temperature and low pressure made possible the observation of strong unimolecular falloff of the dissociation even in this large molecule and the full parametrization of a restricted rotor Gorin model RRKM fit. The choice of restriction parameter η and the average energy transfer $\langle\Delta E\rangle_{down}$ both seem normal. The resulting k_∞ is very close to earlier work that closely represents the high-pressure limit. When combined with other well-known thermochemistry, the barrier estimated from the RRKM extrapolation is 86 kcal/mol and this translates to a heat of formation of 12.8 kcal/mol for *tert*-butyl radical. All aspects of the decomposition are much as expected, and the results are almost routine except for the quite surprising observation of vibrational relaxation in the 25 Torr experiments. The process is fast, with $P\tau < 100$ ns atm, but this is still much slower than the room temperature ultrasonic data, which have $P\tau \sim 4$ ns atm. However, the strong slowing with temperature is easily ascribed to the need to transfer much larger amounts of energy for equilibration at high temperature but with an energy transfer rate already so rapid that it cannot increase much. The relaxation introduces an incubation delay that is quite useful in the modeling of the lowest pressure gradient profiles.

Introduction

The heat of formation of the *tert*-butyl radical has remained a matter of some dispute for several years now. There are roughly two groups of experimental values that spread over 8−12 kcal/mol, but the higher values have recently received some new and independent support from adiabatic ionization energies (15.5 kcal/mol)[1] and electronic structure calculations (13.6).[2] Also, a recent and detailed examination of the *tert*-butyl reaction with HBr[3] resulted in a $\Delta_f H_{298}°$ of 12.4 ± 0.3 kcal/mol.

Many of the experimental estimates of $\Delta_f H_{298}°$ for *tert*-butyl are taken from C−C fission barriers obtained from kinetic studies of neopentane dissociation (see Table 1 for a complete summary till now, and also note Figure 9).

$$C(CH_3)_4 \rightarrow {}^{\bullet}C(CH_3)_3 + CH_3 \qquad (1)$$

Unfortunately, this dissociation is followed by a fast chain reaction carried by both CH_3 and H atom giving an induction time[18] and an inevitable sensitivity to secondary reactions. As usual, most studies of the dissociation are also confined to a rather small range of temperature, as well as to low or moderate pressures, making it difficult to extract an unambiguous E_a^∞ for the high-pressure limit (HPL) from the measurements. The dissociation does seem to be unambiguously reaction 1, but this step is rapidly followed by

$$ {}^{\bullet}C(CH_3)_3 \rightarrow (CH_3)_2C{=}CH_2 + H \qquad (2)$$

further driving the chain. The isobutene product is quite stable and may not dissociate (see below for more on this issue) but will participate in propagation through abstraction as well as in termination of the chain.

TABLE 1: Experimental Determinations of k_1 for Reaction 1

$E_{apparent}$ (kcal mol^{-1})	T range (K)	ref	$E_{apparent}$ (kcal mol^{-1})	T range (K)	ref
78.3	1070−1245	4	80.8	1000−1200	12
85.8	713−823	5	82.0	908−1008	13
80.5	923−1073	6	79.6	945−1016	14
82.0	723−803	7	84.0	1140−1300	15
85.1	793−953	8	62.0	1230−1455	16
78.9	756−845	9	82.0	700−800	17
80.3	1030−1300	10	86.0	1300−1950	present work
84.0	703−743	11			

Although there is a great deal of variation among published rates and derived E_a^∞ for eq 1, there is a fairly tight grouping of magnitudes at the lowest temperatures (700−800 K) where the HPL should apply. This suggests that these results, when combined with some good HPL rates at much higher temperatures, might afford a better estimate of E_a^∞. This notion has motivated the fairly extensive set of laser−schlieren (LS) measurements of the decomposition reported herein. Our rate determinations cover the high temperature range of 1300−1950 K and extend over a wide range of pressures, from 26 to 400 Torr. The low pressures result in a strong and well-defined falloff that allows the parametrization of a rather convincing RRKM model and a solid extrapolation to the HPL. Of course, these experiments also serve to again test weak collision RRKM theory[19] on another unambiguous dissociation of a very large molecule.

Experimental Section

The shock tube used in the experiments has a 4 ft long driver section of 4 in. i.d. connected to a 10 ft driven section of 2.5

* To whom correspondence should be addressed. E-mail: kiefer@uic.edu.

10.1021/jp027224j CCC: $25.00
Published on Web 02/19/2003

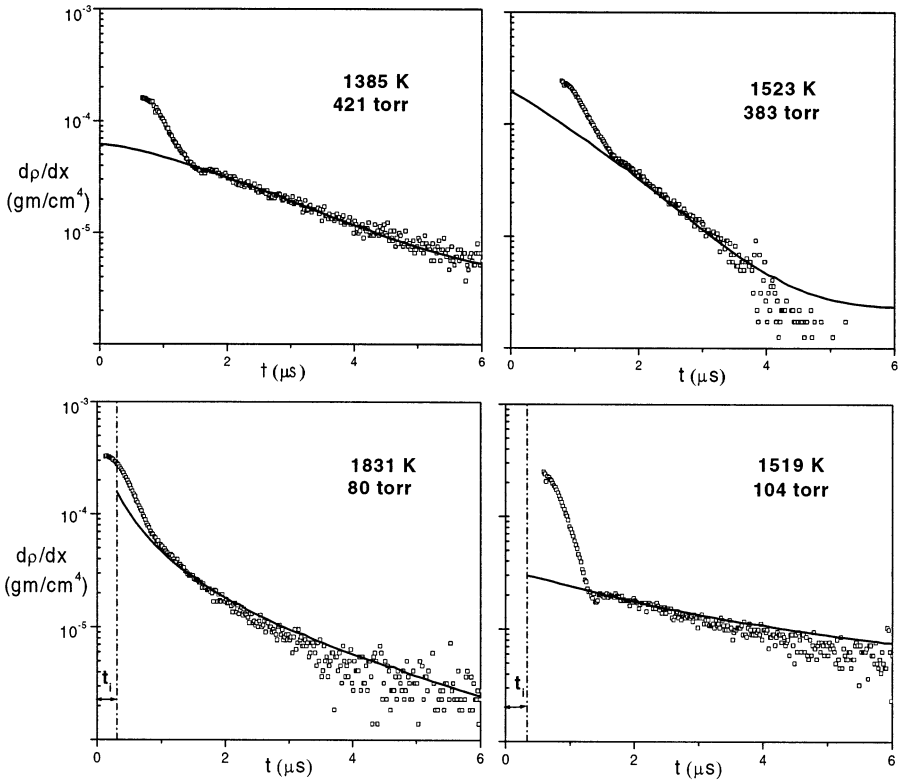

Figure 1. Example dissociation density gradients (□) and modeling of these (solid line) in 2% C_5H_{12}/Kr for moderate to high pressures. Here, temperatures and pressures are all vibrationally relaxed, chemically frozen, ideal incident shock values, values used for the start of modeling. Estimated incubation periods are bounded by the vertical dashed lines with delays marked t_i (see text).

in. i.d., a setup whose details have been fully described.[20] Details of the LS diagnostics have also been given.[21] The data acquisition system for the LS experiment has recently been upgraded, replacing the digitizer with a Gage Electronics Compuscope 12100 PCI card in a PC. The previous digitizer had a maximum sampling rate of 20 MHz and a resolution of 8 bits while the Gage card samples at 50 MHz with 12 bit resolution, resulting in superior process resolution and sensitivity. In addition to the improved hardware, the control and analysis software have also been updated and among other features the software now determines the frozen shock parameters and also calculates the Blythe and Blackman corrections[22] used below in the analysis of vibrational relaxation. As before,[20] velocities were set by interpolation of four intervals centered about the LS beam. On the basis of extensive experience, the uncertainty in velocity is estimated as ±0.2%, corresponding to a temperature error of $<\pm 0.5\%$.

Neopentane was Chemsampco research (99%) grade, and krypton was Spectra Gases excimer grade. The mixtures were prepared manometrically in a 50 L glass vessel and stirred for 2 h using a Teflon-coated magnetic stirrer giving mixtures of 2, 5, 10, 20, and 30% neopentane in krypton. Uncertainties in these compositions are less than ±2%.

To produce the very weak shocks necessary for observation of relaxation, incubation, and falloff in neopentane, a slow flow of driver gas was achieved by introducing various converging−diverging nozzles of different throat diameters at the diaphragm. The present experiments all used Mylar diaphragms of 0.003 or 0.005 in. thickness burst spontaneously with helium. Molar refractivities used in the calculation for density gradient from angular deflection were 25.25 for neopentane and 6.367 for Kr, and these were assumed constant throughout the decomposition. The heat capacities used in the calculation of temperatures and relaxation corrections were taken from the NIST compilation.[23]

Results and Discussion

Dissociation. Example LS profiles of density gradient showing dissociation of the neopentane are shown in Figures 1 and 2. The first set typifies the results of the higher pressure experiments and their modeling, and the second typifies the results for very low pressure. The complete reaction model used in the calculations shown in these figures is listed in Table 2 and discussed below.

Vibrational Relaxation. The very low-pressure experiments of Figure 2 show not only dissociation but also a very short, but definite, preceding vibrational relaxation. Given that relaxation in this molecule at room temperature is already near collision rate, with $P\tau \sim 4$ ns atm,[26] corresponding to $Z_{10} \sim 4$ collisions, a rate that is very much too fast to be resolved in these LS shock wave experiments, this observation was quite unexpected. If these experiments are to be believed, the relaxation time must increase rather strongly with temperature, an "inverted" temperature dependence that is the opposite of nearly all previous measurements of vibrational relaxation in gases[27−29] (the only two extant exceptions appear in the relaxation of norbornene and I_2).[22,30]

The presence of relaxation in the low-pressure experiments is confirmed by examples such as those illustrated in Figures 3 and 4 where both pressure and temperature have been reduced so that dissociation no longer intrudes, and a pure exponential relaxation zone remains evident. Figure 3 displays raw recorded signals whereas Figure 4 has semilog plots of derived density gradient.

A Landau−Teller plot of relaxation times derived from all of our very low-pressure experiments is given in Figure 5. These were derived from the exponential decays seen in semilog plots such as those of Figures 2 and 4 using the standard corrections to molecule time and to the Bethe−Teller relaxation equation

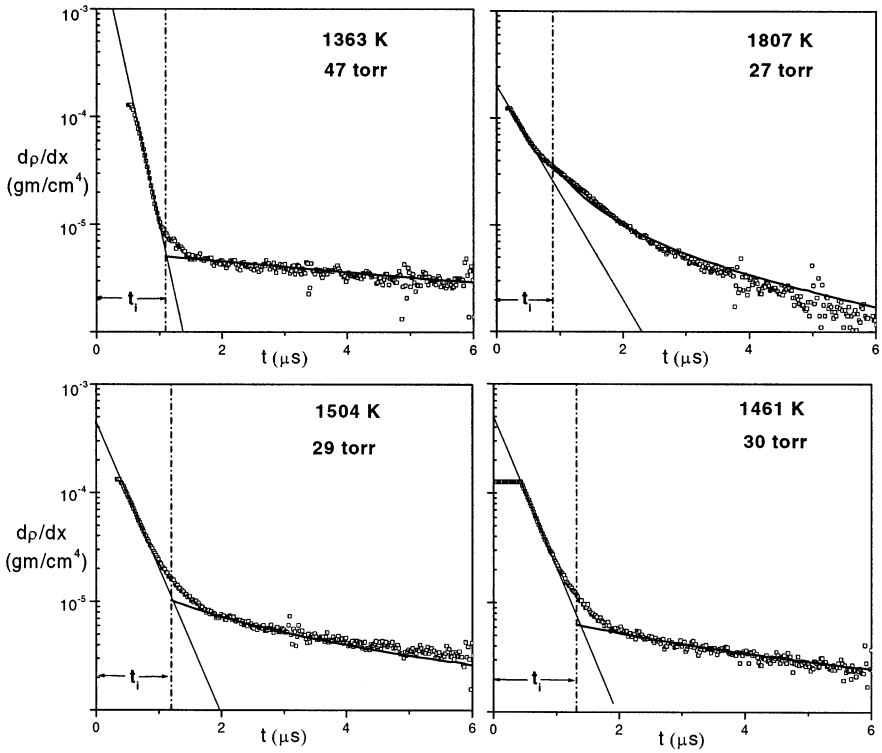

Figure 2. Dissociation and preceding relaxation gradients (□) in 5% C_5H_{12}/Kr at very low pressures. The steep straight lines at the outset are fits of the initial exponential relaxation, and the subsequent curves show modeling of the following decomposition. Estimated incubation periods are bounded by the vertical dashed lines with delays marked t_i. Note the caption of Figure 1.

TABLE 2: Reaction Mechanism for Neopentane Pyrolysis

reaction	log A (cgs)[b]	*n*	*E* (kcal/mol)	source
(1) $C_5H_{12} = CH_3 + H + I\text{-}C_4H_8$[a]	11.040	0.000	46.830	see text
(3) $C_5H_{12} + H = H_2 + CH_3 + I\text{-}C_4H_8$[a]	9.784	1.500	9.370	estimated
(4) $C_5H_{12} + CH_3 = CH_4 + CH_3 + I\text{-}C_4H_8$[a]	1.522	4.000	16.460	estimated
(5) $I\text{-}C_4H_8 = H + C_4H_7$	10.160	0.000	46.000	35
(6) $I\text{-}C_4H_8 + H = H_2 + C_4H_7$	13.600	0.000	7.997	35
(7) $I\text{-}C_4H_8 + CH_3 = CH_4 + C_4H_7$	11.459	0.000	8.843	35
(8) $C_4H_7 = C_3H_{4a} + CH_3$	10.072	0.000	20.000	estimated
(9) $C_3H_{4a} + M = C_3H_{4p} + M$	12.700	0.000	63.000	24
(10) $C_3H_{4a} + H = C_3H_{4p} + H$	13.400	0.000	0.000	24
(11) $M + CH_4 \rightarrow CH_3 + H + M$	17.655	0.000	90.820	24
(12) $CH_4 + H \rightarrow CH_3 + H_2$	14.176	0.000	14.800	24
(13) $CH_3 + CH_3 \rightarrow C_2H_5 + H$	13.500	0.000	14.674	24
(14) $C_2H_5 + M \rightarrow C_2H_4 + H + M$	33.601	−4.990	40.003	24
(15) $2CH_3 \rightarrow C_2H_6$	17.044	−2.100	0.318	see text
(16) $H + C_2H_5 \rightarrow C_2H_4 + H_2$	14.000	0.000	8.000	24
(17) $H + C_2H_6 \rightarrow C_2H_5 + H_2$	9.060	1.500	7.411	24
(18) $CH_3 + C_2H_6 \rightarrow CH_4 + C_2H_5$	−3.260	4.000	8.280	24
(19) $C_2H_4 + M \rightarrow C_2H_3 + H + M$	17.579	0.000	98.157	24
(20) $C_2H_4 + H \rightarrow C_2H_3 + H_2$	6.122	2.530	12.240	24
(21) $CH_3 + C_2H_5 \rightarrow C_2H_4 + CH_4$	13.290	−0.500	0.000	24
(22) $CH_3 + C_2H_4 \rightarrow C_2H_3 + CH_4$	2.418	2.960	8.436	24
(23) $CH_3 + H_2 \rightarrow CH_4 + H$	3.836	2.740	9.418	24
(24) $2C_3H_3 \rightarrow C_6H_6$	12.410	0.000	0.000	24
(25) $C_3H_{4a} + H \rightarrow C_3H_3 + H_2$	6.700	2.000	6.000	24
(26) $2C_3H_3 \rightarrow C_6H_6L$	12.800	0.000	0.000	24
(27) $C_2H_3 + M \rightarrow C_2H_2 + H + M$	41.619	−7.490	45.540	24
(28) $H + C_2H_3 \rightarrow C_2H_2 + H_2$	13.500	0.000	0.000	24
(29) $CH_3 + C_2H_3 \rightarrow C_2H_2 + CH_4$	11.590	0.000	0.000	24
(30) $C_3H_{4a} + M \rightarrow C_3H_3 + H + M$	16.690	0.000	62.300	24
(31) $C_3H_{4p} + M \rightarrow C_3H_3 + H + M$	17.540	0.000	70.400	24
(32) $C_3H_3 + H \rightarrow C_3H_2 + H_2$	13.000	0.000	0.000	24
(33) $C_3H_3 \rightarrow C_3H_2 + H$	12.720	0.000	78.460	24
(34) $H + CH_3 \rightarrow CH_2 + H_2$	13.000	0.000	0.000	25

[a] These reactions include reaction 2. [b] $k = AT^n \exp(-E/RT)$.

previously described and used in the norbornene[22] paper. Although the rates of Figure 5 may be surprisingly slow, they are nonetheless extremely fast, appreciably faster even than those in norbornene and much more rapid than any previously seen in shock waves. The pure relaxation experiments, those that lie below about 1300 K and show no dissociation, also confirm

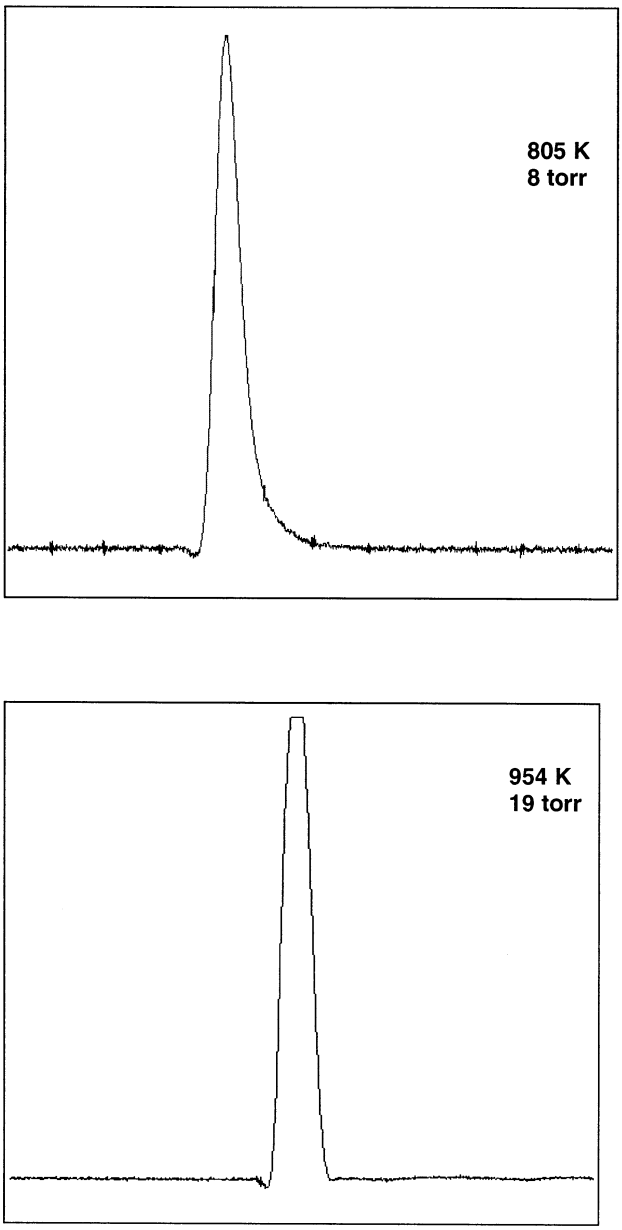

Figure 3. Two examples of LS voltage signals recorded at low temperatures. The upper example shows a well-defined exponential relaxation in 5% C_5H_{12}/Kr, and the lower shows a completely unresolved and undetectable relaxation in 30% C_5H_{12}/Kr.

this inverted temperature dependence, $P\tau$ continuing to decrease as the temperature is lowered.

Unfortunately, as a consequence of the above, the process is soon no longer easily resolved as the temperature is lowered and it is almost impossible to detect below ~600 K. As the temperature approaches this point, the measurement becomes more and more difficult and the results become increasingly unreliable, as indicated by the vagueness of the relaxation zone in the 585 K example of Figure 4 and the increased scatter in the plot of Figure 5 at the lower temperatures. It is also very difficult to resolve the process in mixtures with higher neopentane fractions, a consequence of the shock relations. The increased heat capacity requires stronger shocks to reach the necessary high temperatures, and these inevitably have larger velocities and density ratios. As illustrated in the lower example of Figure 3, this produces a strong time compression and a corresponding loss of resolution. Nonetheless, it was possible to resolve relaxation with some variation of the neopentane fraction, and the data of Figure 5 show no indication of composition dependence.

The observation of relaxation in neopentane in these high-temperature shock waves was certainly unexpected and with the implied inverted temperature dependence may seem quite anomalous, but it is actually not surprising. As shown below and elsewhere,[31] it is a consequence of energy transfer that is already so efficient that it occurs on almost every collision at room temperature, so it simply cannot get much faster. The relaxation time then increases with temperature because of the need to ultimately transfer much larger amounts of energy at high temperatures. This notion is clearly if crudely embodied in the familiar relation[27,28]

$$P\tau = (C_v^{vib}/C_v^{1})RT/P_{10}Z_c(1 - \exp -h\nu/kT) \qquad \text{(A)}$$

Here C_v^1 is the heat capacity of the lowest frequency mode (200 cm^{-1}) and $h\nu$ is its energy. C_v^{vib} is that of the entire molecule. Their ratio is the familiar correction suggested by the "series" model in which all modes relax through and in concert with the lowest mode. Z_c is the collision rate constant. P refers to the pressures (atm), τ refers to the relaxation times (ns), h is Plank's constant, T is the temperature (K), k is Boltzmann's constant, R is the universal gas constant, and ν is the vibrational frequency (cm^{-1}). Except for Z_c and perhaps the transition probability P_{10}, everything in eq A increases with T; for a constant P_{10}, the net increase is very roughly like T^2. This theory is of course crude at best, and without further information on the actual variation of P_{10}, even this notion cannot be made quantitative, but the result does agree with the trend in Figure 5 if P_{10} about doubles—from 0.25 to 0.5—over 300−1800 K. This explanation is of course consistent in a general way with the other examples of inverted temperature dependence, norbornene and I_2,[22,30] where relaxation is again very fast at low temperatures.

Incubation Times. For the present work, with its emphasis on dissociation, the most important feature of the resolved relaxation is actually the accompanying incubation time, a delay in the onset of dissociation while the molecule relaxes to a steady state distribution.[32] In the examples of Figure 2, the reaction then does not begin at the putative time origin, i.e., at the actual shock front, but rather at about the point where the relaxation and dissociation gradients become the same. This point is identified in each of Figure 2. The location in these figures is not sharp both because the transition to steady dissociation is not instantaneous and the profile is smoothed by the finite width of the laser beam. It would be difficult to separate these effects.

The above situation is actually very advantageous for the extraction of a good rate constant at low pressures. At the extremely low pressures of Figure 2, i.e., below ~30 Torr, the shock front becomes increasingly curved and the diffraction/interference contribution to its signal, and the consequent initial negative signal in LS profiles, simply disappears. It is then very difficult to set a good time origin, but the incubation makes this unnecessary. The reaction now begins near the end of the incubation period, a much more clearly identified point in the gradient profile. As seen in Figure 2, the computed decomposition gradients are positioned to begin at this point, some considerable time after the time origin.

In fact, without the introduction of such a delay, it is quite impossible to fit these profiles. If the modeling is taken to begin at the time origin, a much larger initial rate is necessary because the gradient then rapidly decreases—from both temperature drop and loss of reactant—and ends up well below the later measure-

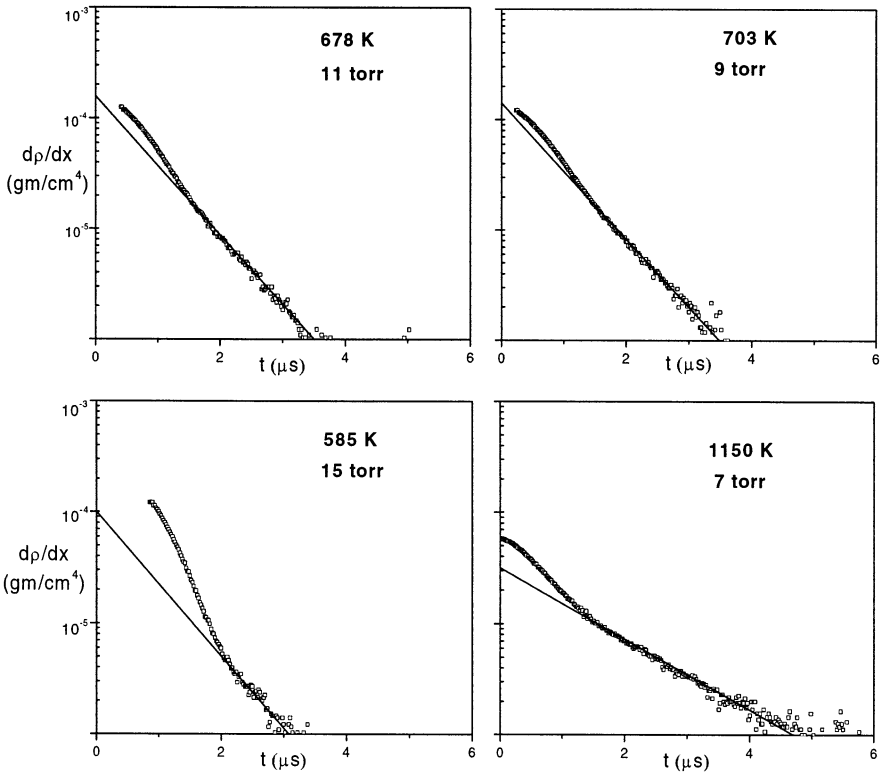

Figure 4. Semilog plots of relaxation in low *T*, low *P* experiments with no evident decomposition. The exponential relaxation zone is fit and emphasized by the solid lines; preceding signals arise from shock front refraction. In the 585 K example, this refraction signal extends over 2 s, simply because the shock is so very slow. Again, note Figure 1.

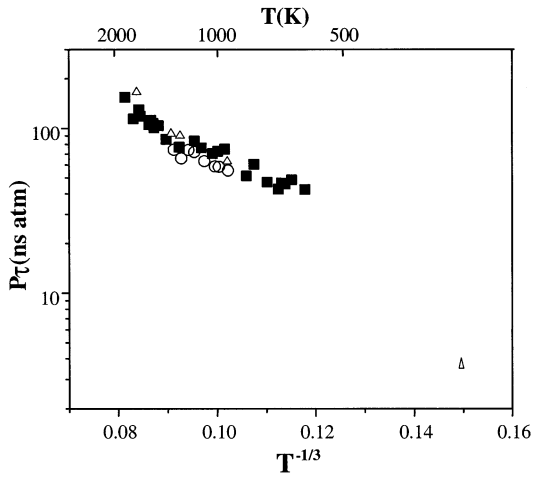

Figure 5. Landau−Teller plot of vibrational relaxation times for 5% C_5H_{12}−Kr (■), 10% C_5H_{12}−Kr (○), and 20% C_5H_{12}−Kr (△). The single point (□) at 300 K is for pure C_5H_{12}, taken from ref 25.

ments. As demonstrated in Figure 6, an incubation delay is simply a necessity for modeling these data.

Unfortunately, the rapidity of the relaxation and the large uncertainty in time−origin location obviate any attempt to compare relaxing density change from the experiments with thermodynamic values, and no such attempt is made herein. The same difficulties occur in setting values for the incubation times, although they are much less sensitive. Some estimates are needed for analysis of the intermediate pressure experiments, so a set of best values are shown in Figure 7, where the t_i/τ ratios are seen to be similar to those in norbornene.[22] There is a slight effect of incubation on the highest temperature experiments at 100 Torr (note the example in Figure 1 at 1831 K). The small incubation times introduced there were estimated from the very low-temperature values of Figure 1 assuming a second-order dependence.

Mechanism. The neopentane decomposition is a fast chain reaction, often with major property and composition variations even in the short LS time period. Thus, extraction of a dissociation rate requires the use of a rather extensive mechanism to ensure that all secondary contributions to the decomposition gradient are properly included. The detailed mechanism used here is listed in Table 2. For each reaction, the source of rate is indicated in the table. To match experimental gradients, only two reactions were arbitrarily adjusted, the dissociation, reaction 1, and occasionally the recombination of CH_3, reaction 15. The latter can make an important contribution to the late time gradient, especially for high pressures where these late gradients can become very small or even slightly negative from this exothermic third-order process (note the small gradient late in the Figure 1 example at 1523 K). The difficulty with this latter reaction lies in the pressure and temperature dependence of its recombination rate, a dependence that is just not unambiguously established by earlier work for these extreme conditions. These experiments are clearly not the way to determine the rate of this process, and attempts to adjust the rate so as to accurately match the late gradients at high pressures were abandoned. There is little effect on the early gradients, and thus the dissociation rate, in any case.

The thermochemistry required here is quite straightforward, because the only problematic radicals, neopentyl [33] and *tert*-butyl,[34] are so unstable that they may be considered to dissociate instantly. Then, their dissociation reactions may be combined with the reactions that form them into a single overall process, as has been done here with reactions 1, 3, and 4. The *i*-butenyl radical (C_4H_7) formed by H atom loss from isobutene is more stable and was treated separately (reaction 8), and the effect of its possible slow dissociation was monitored. In general,

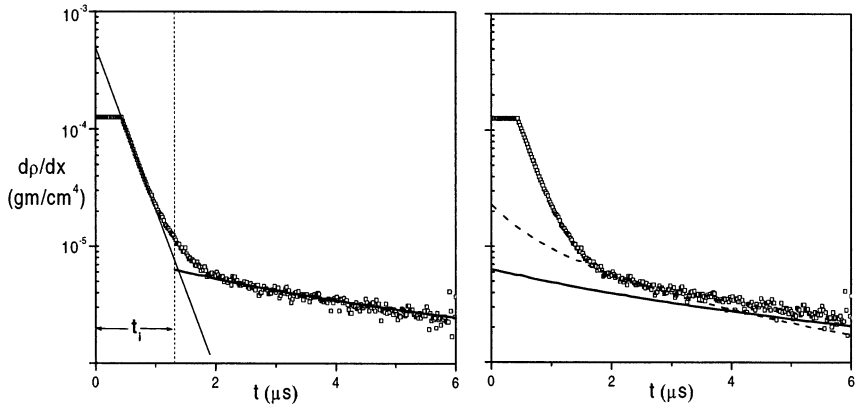

Figure 6. Example illustrating the need for incubation delay in modeling the low-pressure class of experiments. The first figure is a repetition of the 1461 K example in Figure 2, and the second shows two attempts to model without incubation. Neither is considered satisfactory.

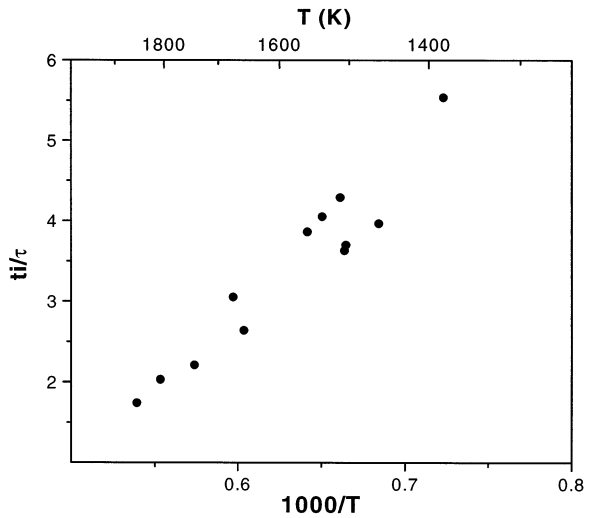

Figure 7. Incubation times in 5% C_5H_{12}−Kr (●).

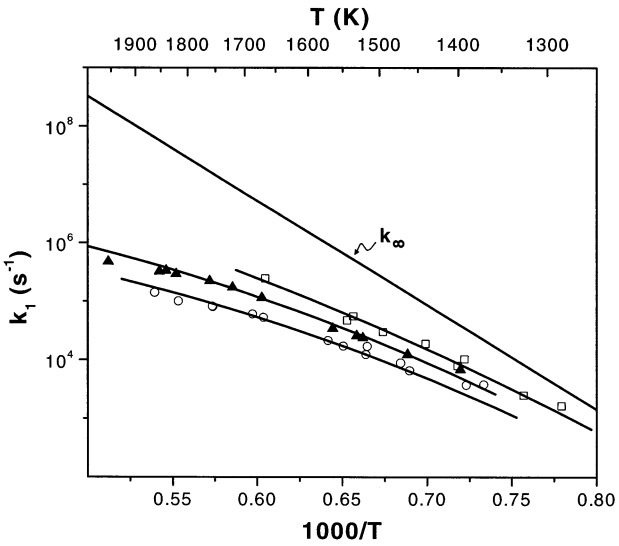

Figure 8. Rate constants for C−C fission in 5% C_5H_{12}−Kr mixture (○), 20−30 Torr; 2% C_5H_{12}−Kr mixture (▲), 80−110 Torr; 2% C_5H_{12}−Kr (□), 370−430 Torr. The RRKM model fit is shown by the solid lines for 25, 100, and 400 Torr, respectively.

thermochemical data were taken from the NIST compilation of S. E. Stein.[23]

On the whole, the model works quite well, especially at short times where dissociation dominates, and the short time gradients are really not sensitive to much beyond reaction 1. For example, in the 1461 K shock of Figure 2, the gradient is more than 90% from reaction 1 out to 6 μs. However, at higher pressure and/or temperature, other reactions, mainly H atom abstraction from isobutene and the combination of CH_3 and H to methane, do begin to affect the gradient. Nonetheless, even in the most extreme example of Figure 1 at 1831 K, the gradient is still more than 75% from reaction 1 out to 3 μs, and the sensitivity to reaction 1 is actually much higher than this because the lesser contributors are tied to it. Despite the complications introduced by radical formation and the resulting chain decomposition, these experiments still provide a very direct and unambiguous measure of the rate of the dissociation, reaction 1.

There is little information on the reactions of isobutene and none for these conditions, so the assigned rates are taken from a parallel study of its pyrolysis with the LS technique under comparable conditions.[35] For one thing, this study shows that the direct dissociation of isobutene, reaction 5, is too slow to make much of a contribution for present conditions; the important reaction is rather the abstraction reaction 8, and this is also taken from the isobutene pyrolysis study. Details of this study will be published elsewhere.[35]

Rate constants for reaction 1 were derived from the gradient records by a process of iteration, the rate being varied for each experiment until an overall satisfactory agreement was achieved. The resulting rate constants are displayed in Figure 8, where they are accompanied by a RRKM modeling. To save effort, when only minor further adjustment was indicated, small additional changes were made in the dissociation rates used in modeling when experience so indicated, and the adjusted rates were then plotted. Note the example at 1831 K in Figure 1; here, the plotted rate is actually 20% above that in the exhibited simulation.

The measured rates of Figure 8 appear to form a quite consistent set, and both magnitude and slope are well-defined. It should be recognized that the deviation of the two lowest temperature points from the RRKM fit to the lowest pressure data need not be significant. Here, the gradients are very small and boundary layer signals may intrude. Probable errors are discussed below.

RRKM Model. As is quite evident in Figure 8, there is severe falloff in the measured rates, especially in those at the lowest pressures. At such pressures and temperatures, both magnitude and apparent E_a are greatly reduced from their likely high-pressure values. Determination of an E_a^∞ clearly requires a significant extrapolation, and RRKM theory has been used for this purpose.

The RRKM model whose results are displayed in Figure 8 is the restricted rotor Gorin model[16] delineated in Table 3. Most

TABLE 3: Restricted Rotor Gorin Model RRKM Parameters for $C_5H_{12} \rightarrow C_4H_9 + CH_3$

frequencies (cm^{-1}) and degeneracies		
C_5H_{12}[a]	2970(2), 2968(3), 2966(3), 2860(4), 1480(3), 1462(5), 1405(1), 1377(3), 1276(3), 1016(2), 972(3), 901(3), 729(1), 400(3), 334(2), 210(3), 200(1)	
C_4H_9[a]	2971(2), 2966(1), 2933(3), 2833(3), 1458(3), 1454(2), 1453(1), 1368(2), 1330(1), 1261(2), 1003(1), 925(2), 904(3), 751(1), 422(2), 158(1), 119(2), 115(1)	
CH_3[a]	3162(2), 3044(1), 1396(2), 607(1)	
moments of inertia ($\times 10^{-40}$ g cm^2)		
molecular active	165.0	ref 12
transition state active	2.923, 2.923, 5.864, 88.0, 88.0, 176.0	estimated
η	1 − (0.003)	present work
E_o (=$\Delta H_0°$) (kcal/mol)	86.000	present work
$(\Delta E)_{down}$ (cm^{-1})	750.0	present work

[a] For vibrational frequencies, see ref 16. The state count used a grain size of 10 cm^{-1}. The methyl rotors are treated as vibrations, even for energies above threshold. The rotational barrier (4.7 kcal/mol[41]) is too high for this to contribute.

of this, the vibration frequencies for the transition state and some moments of inertia, are those used by Baldwin, Lewis, and Golden[12] in their earlier treatment of the same problem. To match the data, E_o (the barrier), η (the restriction parameter), and $\langle\Delta E\rangle_{down}$ (the average energy transferred in deactivating collisions) were adjusted to produce the agreement shown in Figure 8. The chosen optimum values for these are also given in Table 3. Lowering the barrier and readjusting the other two might better fit the lowest pressure results, but then the high-pressure slope is too shallow. It may be difficult to set an accurate E_o with these data alone, but the magnitude seems quite solid. Some trials suggest that k_∞ cannot be altered by more than an average ±30%, but it is impossible to prove the point.

Our best estimate of the HPL rate is finally (1300−2000 K)

$$\log k_\infty \text{ (cm}^3\text{/mol s)} = 28.545 - 3.070 \log T - 90.93/2.3RT$$

A comparison of literature rates for reaction 1 with our k_∞ is made in Figure 9. In general, agreement is quite good; for example, we agree very closely with the HPL extrapolation of Baldwin et al.,[12] and the other high-temperature rates may well rise somewhat on extrapolation to this limit. As usual, we find the results of Rao and Skinner[16] to be too low.[36,37]

Despite the severe falloff seen in the lowest pressure experiments, the falloff curve is too broad to allow a close approach to the LPL. Even for the most extreme conditions (2000 K, 25 Torr), the RRKM model still has the effective second-order rate constant an order of magnitude below the LPL value.

***tert*-Butyl Heat of Formation.** As noted in the Introduction, it is now possible to combine this very high-temperature k_∞ with the best low-temperature rate data to derive an improved E_a^∞ and barrier. These low-temperature experiments are essentially at the HPL, as is indicated by our RRKM model. This model already agrees with the higher values among the 700−800 K rate data as seen in the summary comparison of Figure 9 (that of ref 5, in particular), so we have made no further alterations. Our best barrier estimate is thus 86 kcal/mol; if agreement with the smaller of the low-temperature rates was to be preferred, this E_o would of course increase. We use $H_{298}° - H_o° = 4.300$ kcal/mol[2] for *tert*-butyl and 2.487[24] and 4.239 kcal/mol for methyl and neopentane. Then, $\Delta H_{298}°$ for reaction 1 is 88.55 kcal/mol. Combining with $\Delta_f H_{298}° = -40.13$[38] and 35.6[38] kcal/mol for neopentane and methyl, respectively, we finally have $\Delta_f H_{298}°$ for *tert*-butyl = 12.80 kcal/mol.

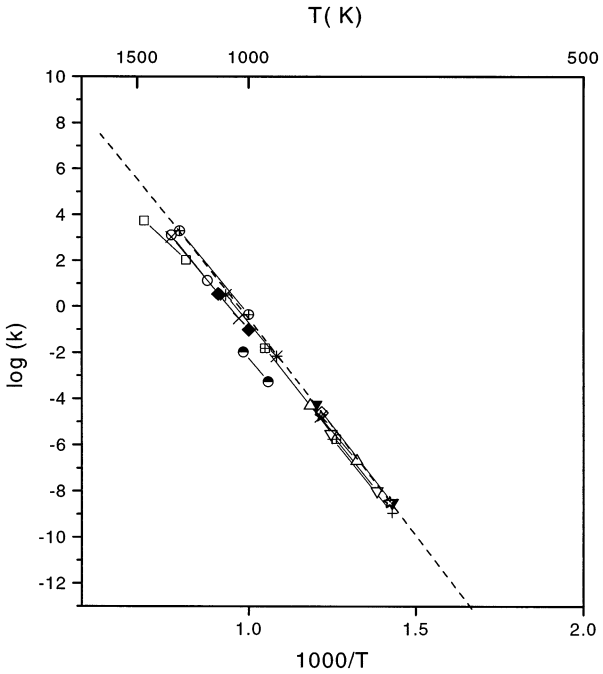

Figure 9. Comparison of present derived k_∞ (- - -) with earlier literature rates listed in Table 1. Ref 4 (◆), ref 5 (▼), ref 6 (*), ref 7 (▽), ref 8 (⊡), ref 9 (△), ref 10 (×), ref 11 (☆), ref 12 (⊗), ref 14 (◓), ref 15 (○), ref 16 (□), and ref 17 (+).

Conclusions

The dissociation/decomposition of neopentane was examined at very high temperatures and over a very wide range of pressure in a shock tube using the LS technique. The combination of high temperature and low pressure makes possible observation of a strong unimolecular falloff in this large molecule and the full parametrization of a restricted rotor Gorin model RRKM fit. The choice of restriction parameter η and the average energy transfer $\langle\Delta E\rangle_{down}$ seems normal. The resulting k_∞ is very close to the earlier extrapolation of Baldwin and Golden (see Figure 9) and to the large collection of lower temperature rates, rates that must closely approximate k_∞. When combined with well-known thermochemistry, our barrier of 86 kcal/mol translates to a heat of formation of 12.8 kcal/mol for *tert*-butyl radical.

The $\Delta_f H_{298}°$ = 12.8 kcal/mol for *t*-butyl derived here lies at the high end of published values but is very close to the most recent estimates—both the electronic structure theory result of 13.6[2] and the experimental 12.4 obtained from the study of bromination equilibria by Seetula and Slagle.[3] Comparing other rate-derived results, we note that had Baldwin and Golden[12] combined their higher temperature HPL extrapolation with the available 700−800 K data as was done here, rather than relying on an E_a derived from their own limited temperature range, they would have quantitatively agreed with the present conclusion.

It is really quite impossible to set error limits on the above $\Delta_f H_{298}°$. Although there is of course some uncertainty in the LS data and also in the low-temperature experiments used to extend the temperature range, it seems that the major uncertainty here must lie in the RRKM model. This uncertainty is not so much from the extrapolated k_∞, either its E_a or A factor, but rather in the temperature dependence of the A factor. The model used here assumes a temperature-independent restriction parameter, but other choices are certainly possible,[12,16] and any change will require a compensating adjustment in E_o to retain

the fit. When E_a is forced to be E_o, the temperature dependence of the A factor in our k_∞ is very roughly T^2. This could well be a factor of T either way, so we conclude that it is impossible to set E_o to better than about ± 2 kcal/mol. We thus propose $\Delta_f H_{298}^\circ$ (*tert*-butyl) $= 12.8 \pm 2$ kcal/mol. The extraction of a more solid value will require a more refined and convincing treatment of the bond−fission transition state.[39,40]

The dissociation study reported here has no real surprises. The experiments and their modeling require only quite standard theory, and the description it provides is excellent. The one surprising observation is vibrational relaxation of the neopentane in the lowest pressure experiments, with $P\tau$ values as high as 100 ns atm near 1700 K. Considering that $P\tau$ is ~ 4 ns atm ($Z_{10} \sim 4$) at room temperature in this molecule, this implies a fairly strong negative or inverted temperature dependence, and such has rarely been seen. However, the result is perhaps not so surprising. It is still very fast and may just reflect the much greater vibrational energy that has to be provided at high temperature through a process that already is so fast that it cannot measurably increase in rate. This effect is already embodied in routine equations used in the analysis of earlier ultrasonic studies and may well be quite general. Thus, it may well be that at such very low pressures, nothing is really too fast; the LS technique can actually resolve relaxation in virtually any molecule at high temperatures when it is at least somewhat dilute in a rare gas. This suggestion may seem a bit strong, but it now seems to be tenable. As of this writing, it already has considerable additional support that will be examined more fully in subsequent publications.[31,35] For now, we observe that its important consequence for any future dissociation study is the introduction of an incubation time, a delay in the onset of reaction that allows one to bypass the difficulty of time origin location in extremely low-pressure experiments. We plan to exploit this discovery to further delineate falloff effects in large species.

Acknowledgment. The support of the U. S. Department of Energy, Division of Basic Energy Sciences, under Grant No. DE-FG02-85ER13384 is gratefully acknowledged.

References and Notes

(1) Houle, F. A.; Beauchamp, J. L. *J. Am. Chem. Soc.* **1979**, *101*, 4067.
(2) Smith, B. J.; Radom, L. *J. Phys. Chem. A* **1998**, *102*, 10787.
(3) Seetula, J. A.; Slagle, I. R. *J. Chem. Soc., Faraday Trans.* **1997**, *93*, 1709.
(4) Tsang, W. *J. Chem. Phys.* **1966**, *44*, 4283.
(5) Halstead, M. P.; Konar, R. S.; Leathard, D. A.; Marshall, R. M.; Purnell, J. H. *Proc. R. Soc. London A* **1969**, *310*, 525.
(6) Taylor, J. E.; Hutchings, D. A.; Frech, K. J. *J. Am. Chem. Soc.* **1969**, *91*, 2215.
(7) Baronnet, F.; Dzierzynski, M.; Come, G. M.; Martin, R.; Niclause, M. *Int. J. Chem. Kinet.* **1971**, *3*, 197.
(8) Pacey, P. D. *Can. J. Chem.* **1973**, *51*, 2415.
(9) Marshall, R. M.; Purnell, H.; Storey P. D. *J. Chem. Soc., Farady Trans. 1* **1976**, *72*, 85.
(10) Bradley, J. N.; West, K. O. *J. Chem. Soc., Faraday Trans. 1* **1976**, *72*, 8.
(11) Marquaire, P. M.; Come, G. M. *React. Kinet. Catal. Lett.* **1978**, *9*, 171.
(12) Baldwin, A. C.; Lewis, K. E.; Golden, D. M. *Int. J. Chem. Kinet.* **1979**, *11*, 529.
(13) Azay, P.; Come, G. M. 177th American Chemical Society National Meeting; 38th Chemical Society of Japan National Meeting, Honolulu, Hawaii, 1979.
(14) Pratt, G. L.; Rogers, D. *J. Chem. Soc., Faraday Trans. 1* **1981**, *77*, 2751.
(15) Bernfeld, D.; Skinner, G. B. *J. Phys. Chem.* **1983**, *87*, 3732.
(16) Rao, V. S.; Skinner, G. B. *Int. J. Chem. Kinet.* **1988**, *20*, 165.
(17) Mitchell, T. J.; Benson, S. W. *Int. J. Chem. Kinet.* **1993**, *25*, 931.
(18) Pacey, P. D.; Wimalasena, J. H. *Chem. Phys. Lett.* **1978**, *53*, 593.
(19) Kiefer, J. H. *Twenty-Seventh Symposium (International) on Combustion*, The Combustion Institute, 1998; p 113.
(20) Kiefer, J. H.; Manson. A. C. *Rev. Sci. Instrum.* **1981**, *52* (9), 1392.
(21) Kiefer, J. H. In *Shock Waves in Chemistry*; Lifshitz, A., Ed.; Marcel Dekker: New York, 1981; pp 219−277.
(22) Kiefer, J. H.; Kumaran, S. S.; Sundaram, S. *J. Chem. Phys.* **1993**, *99* (5), 3531. (Note: The blythe correction factor given here is incorrect. The correct expression is $\mu = C_{vib}/C_\alpha[1 - (m^2(\gamma_\alpha - 1)/(1 - m^2))]$. The correct expression was used therein; this paper simply seems to have a transcription error.)
(23) Stein, S. E.; Rukkers, J. M.; Brown, R. L. NIST Standard Reference Database 25. *Thermochemical Data*, Version 1.2; NIST: Gaithersburg, MD, 1991.
(24) Ikeda, E.; Tranter, R. S.; Kiefer, J. H.; Kern, R. D.; Singh, H. J.; Zhang, Q. *Proc. Combust. Inst.* **2000**, *28*, 1725.
(25) Kiefer, J. H.; Kumaran, S. S. *J. Phys. Chem.* **1993**, *97*, 414.
(26) Holmes, R.; Jones, G. R.; Lawrence, R. *Trans. Faraday Soc.* **1965**, *62*, 46.
(27) Cottrell, T. L.; McCoubrey, J. C. *Molecular Energy Transfer in Gases*; Butterworths: London, 1961.
(28) Stevens, B. Collision Activation in Gases; *The International Encyclopedia of Physical Chemistry and Chemical Physics*; Pergamon: London, 1967; Vol. 3.
(29) Lambert, J. D.; Salter, R. *Proc. R. Soc.* **1959**, *A253*, 277.
(30) Mcclelland, G. M.; Saenger, K. L.; Valentini, J. J.; Herschbach, D. R. *J. Phys. Chem.* **1979**, *83* (8), 947.
(31) Gireesh, S. C.; Srinivasan, N. K.; Santhanam, S.; Kiefer, J. H. To be published.
(32) Tsang, W.; Kiefer, J. H. Unimolecular Reactions of Large Polyatomic Molecules Over Wide Ranges of Temperature. *Advanced Series in Physical Chemistry 6* (Chemical Dynamics and Kinetics of Small Radicals, Part 1); World Scientific: River Edge, NJ, 1995; pp 58−119.
(33) Tsang, W. *J. Am. Chem. Soc.* **1985**, *107*, 2872.
(34) Warnatz, J. In *Combustion Chemistry*; Gardiner, W. C., Jr., Ed.; Springer-Verlag: New York, 1984.
(35) Santhanam, S.; Kiefer, J. H.; Tranter, R. S. To be published.
(36) Al-Alami, M. Z.; Kiefer, J. H. *J. Phys. Chem.* **1983**, *87*, 499.
(37) Kiefer, J. H.; Shah, J. N. *J. Phys. Chem.* **1987**, *91*, 3024.
(38) Burcat, A.; Mcbride, B. *1995 Ideal Gas Thermodynamic Data for Combustion and Air-Pollution Use*; Technion Aerospace Engineering Report TAE 732; Techni: Haifa, Israel, January 1995.
(39) Pitt, I. G.; Gilbert, R. G.; Ryan, K. R. *J. Phys. Chem.* **1995**, *99* (1), 239.
(40) Wagner, A. F.; Harding, L. B.; Robertson, S. H.; Wardlaw, D. M. *Springer Ser. Chem. Phys.* **1996**, *61*, 203.
(41) Dale, J. *Tetrahedron* **1966**, *22*, 3373.